Supplement of Atmos. Chem. Phys., 22, 8683–8699, 2022
https://doi.org/10.5194/acp-22-8683-2022-supplement

Atmospheric Chemistry and Physics
Open Access

Supplement of

Black carbon aerosol reductions during COVID-19 confinement quantified by aircraft measurements over Europe

Ovid O. Krüger et al.

Correspondence to: Mira L. Pöhlker (poehlker@tropos.de)

Supplementary text

S1 Boundary layer and terrain height below flight track

To provide the planetary boundary layer height below the flight track in figures 6 and A1 we used the HYSPLIT package (Rolph et al., 2017; Stein et al., 2015, version 4, Revision 664, October 2014). We started a new backward trajectory every 60 seconds from the location and altitude of HALO.

The terrain height below the HALO flight track was computed with the online tool GPS visualizer based on the 1 second resolution coordinates of the HALO aircraft (https://www.gpsvisualizer.com/elevation, last access 20.02.2022).

To provide the arithmetic mean of planetary boundary layer and terrain height below the flight track shown in figures 6 and A1 we binned the data along the latitude in $0.2°$ steps. Then we calculated the arithmetic mean for each of these bins.

S2 EUROSTAT data for fossil and solid fuels

Data published by EUROSTAT is used to investigate the reductions in fossil fuel demand during the confinement period in 2020 (https://ec.europa.eu/eurostat/databrowser/view/NRG_JODI__custom_482779/default/table last access 25.01.2021). We use for figures S3, S2, S1, S4 the terminology suggested by EUROSTAT. However, to make these rather technical terms more clear we refer in section 4 to gasoline for motor spirits and aircraft fuel for kerosene. Furthermore, the difference in solid fossil fuel (which is the compilation of hard coal including: anthracite, coking coal and other bituminous coal; brown coal including: sub-bituminous coal and lignite and coal products including: patent fuel, coke oven coke, gas coke, coal tar and brown coal briquettes https://ec.europa.eu/eurostat/statistics-explained/index.php?oldid=449721, last access 19.04.2022) demand between 2017 and 2020 is used to analyze important drivers for the BC reduction, other than the COVID-19 confinements in 2020 (https://ec.europa.eu/eurostat/databrowser/view/NRG_CB_SFF__custom_1131819/default/table?lang=en last access 08.07.2021 and https://ec.europa.eu/eurostat/databrowser/view/NRG_CB_SFFM__custom_1558586/default/table?lang=en last access 12.11.2021).

Supplementary tables

Table S1. Average and median M_{BC} from HALO observations and EMAC simulations. Values in column altitude represent centre of corresponding $500\,\mathrm{m}$ altitude bin.

	EMeRGe EU				BLUESKY					
	Observations		EMAC		Observations		EMAC		EMAC 40 % reduced	
Altitude	Avg	Median	Avg	Median	Avg	Median	Avg	Median	Avg	Median
[m]	[$\mu g\,m^{-3}$]	[$\mu g\,m^{-3}$]	[$\mu g\,m^{-3}$]	[$\mu g\,m^{-3}$]	[$\mu g\,m^{-3}$]	[$\mu g\,m^{-3}$]	[$\mu g\,m^{-3}$]	[$\mu g\,m^{-3}$]	[$\mu g\,m^{-3}$]	[$\mu g\,m^{-3}$]
250	0.083	0.066	0.113	0.113	0.099	0.089	0.156	0.137	0.110	0.097
750	0.172	0.125	0.143	0.128	0.064	0.049	0.109	0.105	0.077	0.073
1250	0.132	0.097	0.119	0.112	0.072	0.056	0.079	0.078	0.056	0.055
1750	0.174	0.106	0.069	0.065	0.045	0.033	0.079	0.086	0.055	0.060
2250	0.119	0.030	0.043	0.030	0.034	0.009	0.031	0.034	0.022	0.024
2750	0.140	0.030	0.044	0.036	0.019	0.006	0.027	0.025	0.019	0.017
3250	0.103	0.047	0.028	0.021	0.012	0.004	0.015	0.010	0.011	0.008
3750	0.023	0.011	0.028	0.019	0.010	0.003	0.011	0.008	0.008	0.006
4250	0.029	0.009	0.010	0.008	0.011	0.005	0.004	0.003	0.003	0.002
4750	0.013	0.005	0.007	0.005	0.008	0.003	0.006	0.003	0.004	0.002

Table S2. Average and median N_{BC} from HALO observations. Values in column altitude represent centre of corresponding $500\,\mathrm{m}$ altitude bin.

	EMeRGe EU Observation		BLUESKY Observation	
Altitude [m]	Avg [cm^{-3}]	Median [cm^{-3}]	Avg [cm^{-3}]	Median [cm^{-3}]
250	41.1	40.3	47.1	48.5
750	81.8	65.4	31.8	27.0
1250	62.5	53.1	33.7	30.7
1750	75.3	52.3	22.9	19.3
2250	54.2	15.0	18.0	5.1
2750	45.0	15.6	8.6	3.5
3250	34.4	25.8	4.7	2.4
3750	10.2	6.0	4.1	2.4
4250	10.8	4.7	4.2	3.2
4750	4.6	2.9	3.2	2.6

Table S3. Average and median of M_{BC} microphysical properties, geometric mean diameters (D_{rBC}) and the geometric standard deviation (σ_{rBC}) of the core size distributions. Values in column altitude represent centre of corresponding $500\,\mathrm{m}$ altitude bin.

	EMeRGe EU				BLUESKY			
	D_{rBC}		σ_{rBC}		D_{rBC}		σ_{rBC}	
Altitude	Avg	Median	Avg	Median	Avg	Median	Avg	Median
[m]	[nm]	[nm]			[nm]	[nm]		
250	157	155	2.083	2.047	144	152	2.180	2.063
750	167	150	2.006	1.966	134	140	2.268	2.108
1250	171	172	1.924	1.900	148	150	2.149	2.124
1750	174	157	1.872	1.858	138	138	2.027	1.972
2250	150	148	1.826	1.789	125	122	1.917	1.954
2750	155	153	1.749	1.714	151	165	1.866	1.907
3250	159	158	1.808	1.803	115	134	1.731	1.642
3750	169	174	1.701	1.735	130	134	1.642	1.634
4250	174	178	1.645	1.663	157	157	1.444	1.444
4750	170	160	1.447	1.463	157	148	1.392	1.405

Table S4. Vertically integrated M_{BC} burden per surface area. BLUESKY adjusted is the BLUESKY observation and the EMAC model retrieved adjustment (see section 2.4). Values in column altitude represent centre of corresponding $500\,\mathrm{m}$ altitude bin. Pressure altitude scaling factor calculated as described in section A4. Last row provides column sum of vertically integrated M_{BC} burden.

Altitude [m]	Pressure altitude scaling factor	EMeRGe EU Median [$\mu\mathrm{g\,m^{-2}}$]	BLUESKY Median [$\mu\mathrm{g\,m^{-2}}$]	BLUESKY Adjusted Median [$\mu\mathrm{g\,m^{-2}}$]
250	1.03	31.86	43.00	31.23
750	1.09	57.14	22.40	32.87
1250	1.16	41.51	24.26	38.88
1750	1.24	42.88	13.19	4.97
2250	1.32	11.48	3.49	1.89
2750	1.40	10.71	2.01	5.84
3250	1.49	15.86	1.18	4.70
3750	1.59	3.52	1.09	4.61
4250	1.70	2.75	1.36	2.67
4750	1.81	1.31	0.88	1.28
Sum		219.04	112.86	128.95

Supplementary figures

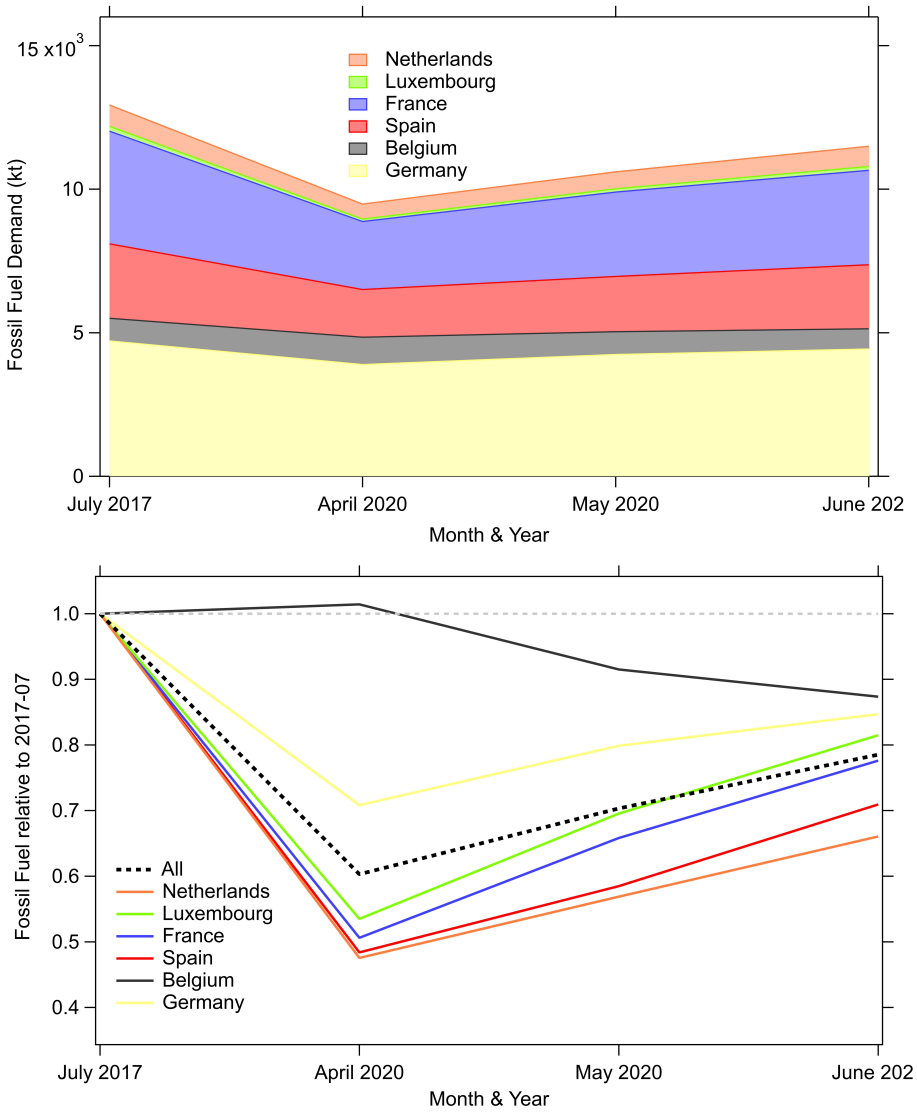

Figure S1. Cumulative EUROSTAT data for fossil fuel demand for the July 2017, April 2020, May 2020 and June 2020. The data combines demand for diesel, kerosene (aviation fuel) and motor spirit (gasoline). Data is downloaded for countries considered in this study from the EUROSTAT website with last access 08.07.2021 (https://ec.europa.eu/eurostat/databrowser/view/NRG_CB_SFF__custom_1131819/default/table).

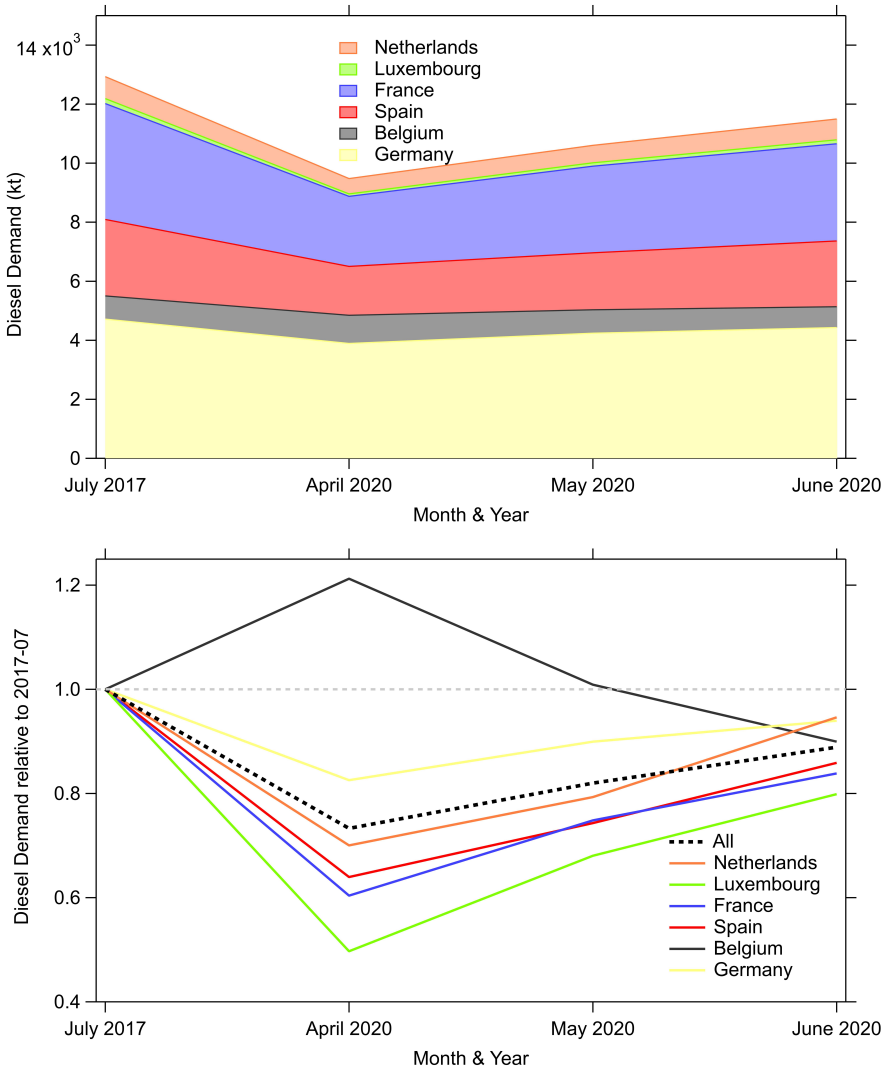

Figure S2. Cumulative EUROSTAT data for diesel demand for July 2017, April 2020, May 2020 and June 2020. Data is downloaded for countries considered in this study from the EUROSTAT website with last access 08.07.2021 (https://ec.europa.eu/eurostat/databrowser/view/NRG_CB_SFF__custom_1131819/default/table).

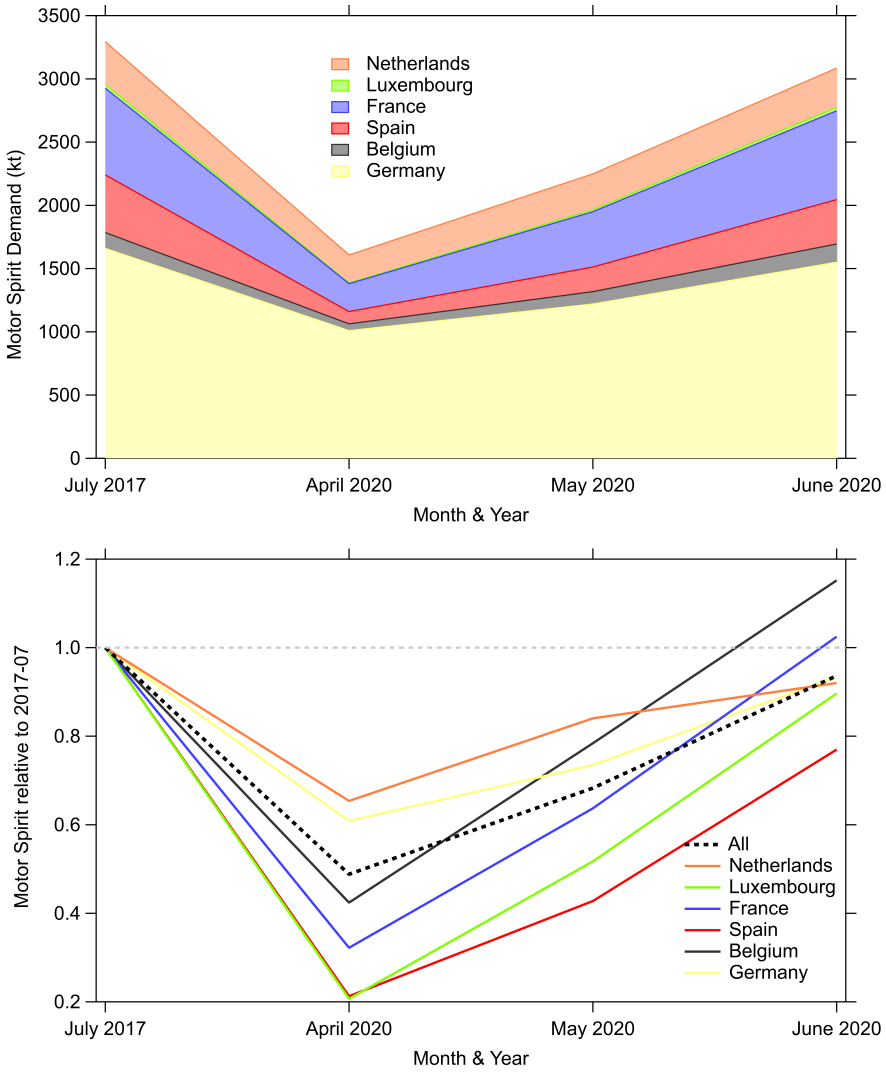

Figure S3. Cumulative EUROSTAT data for motor spirit (gasoline) demand for the July 2017, April 2020, May 2020 and June 2020. Data is downloaded for countries considered in this study from the EUROSTAT website with last access 08.07.2021 (https://ec.europa.eu/eurostat/databrowser/view/NRG_CB_SFF__custom_1131819/default/table).

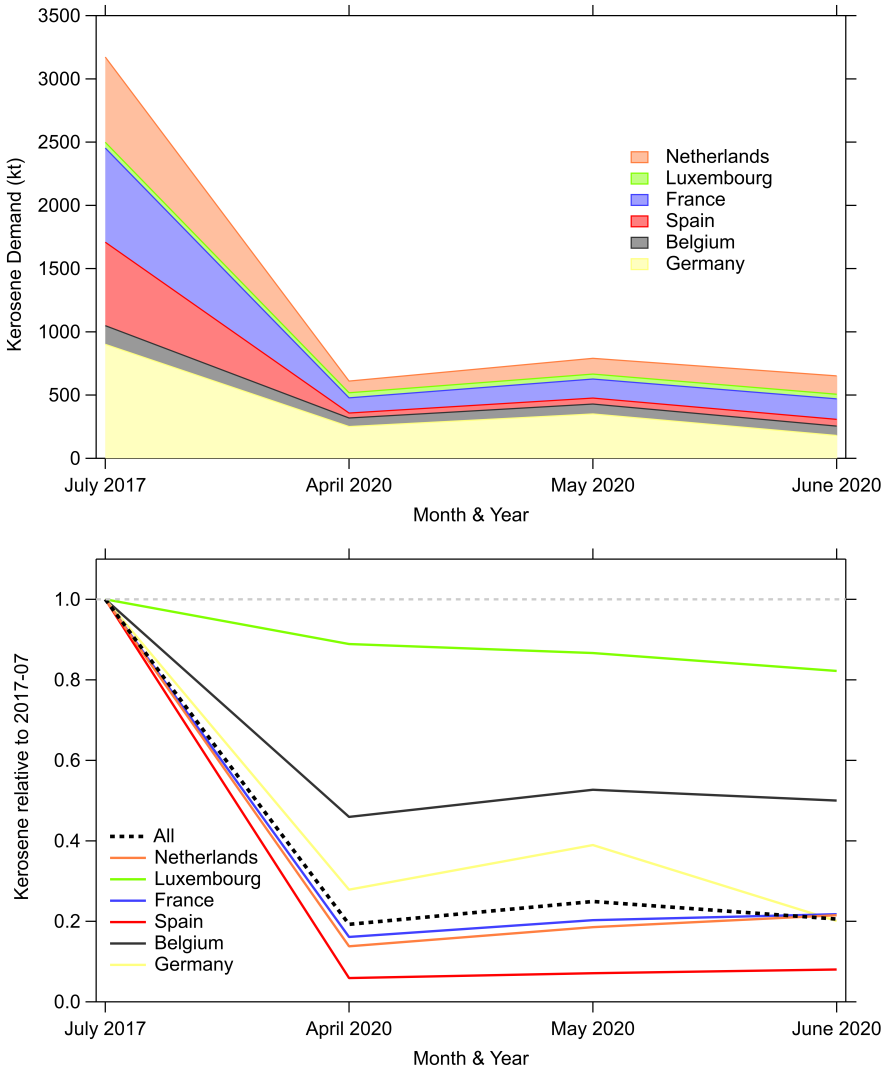

Figure S4. Cumulative EUROSTAT data for kerosene (aviation fuel) demand for the July 2017, April 2020, May 2020 and June 2020. Data is downloaded for countries considered in this study from the EUROSTAT website with last access 08.07.2021 (https://ec.europa.eu/eurostat/databrowser/view/NRG_CB_SFF__custom_1131819/default/table).

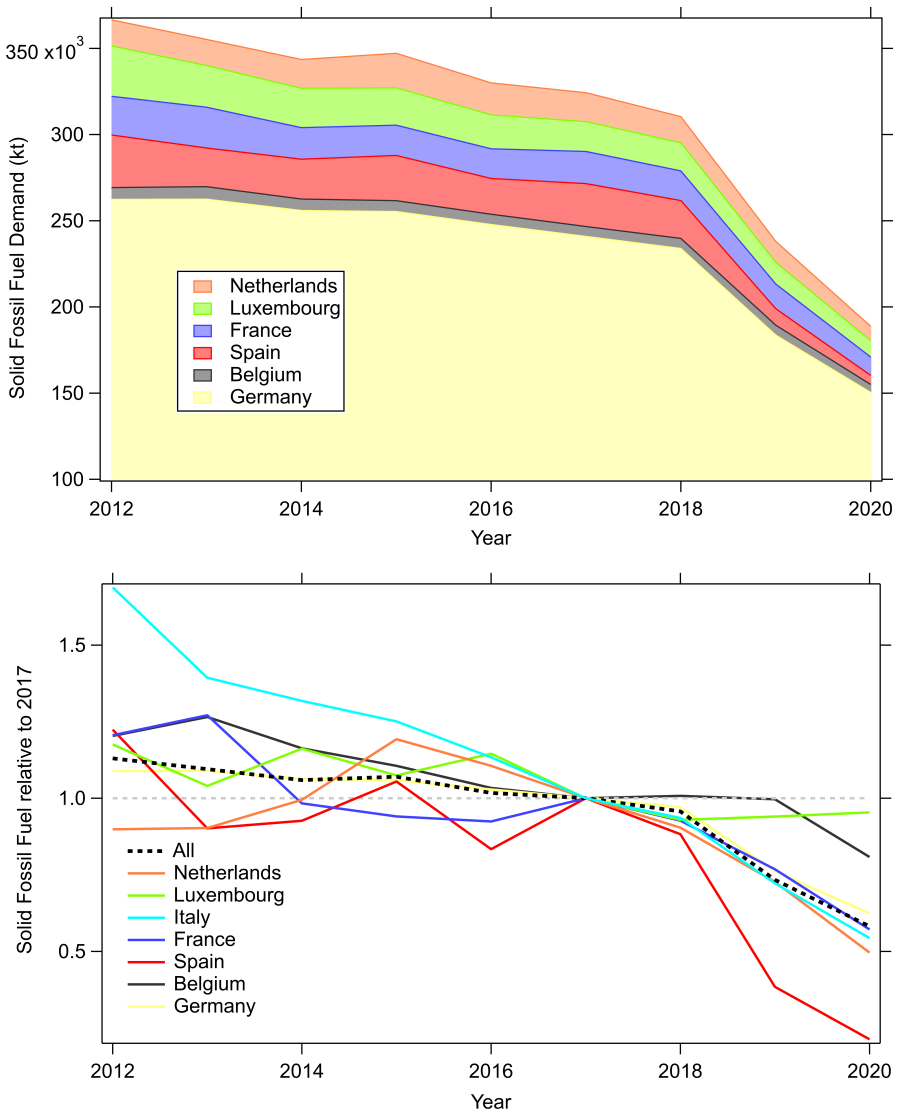

Figure S5. Cumulative EUROSTAT data for solid fossil fuel inland consumption for the years 2012 to 2020. Data is downloaded for countries considered in this study from the EUROSTAT website with last access 08.07.2021 (https://ec.europa.eu/eurostat/databrowser/view/NRG_CB_SFF__custom_1131819/default/table).

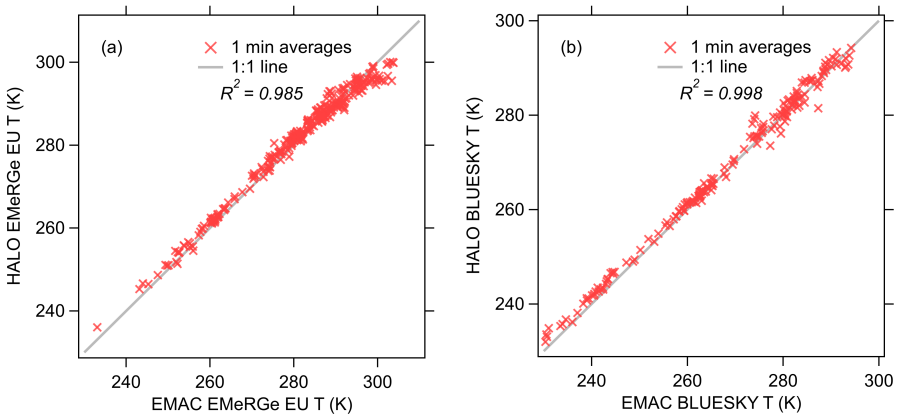

Figure S6. Scatter plot for ambient temperature (T) in K from HALO measurements and EMAC model simulations. Grey line is the one to one ratio. (a) corresponds to measurements from 2017 with R^2 = 0.985. (b) are 2020 measurements with R^2 = 0.998.

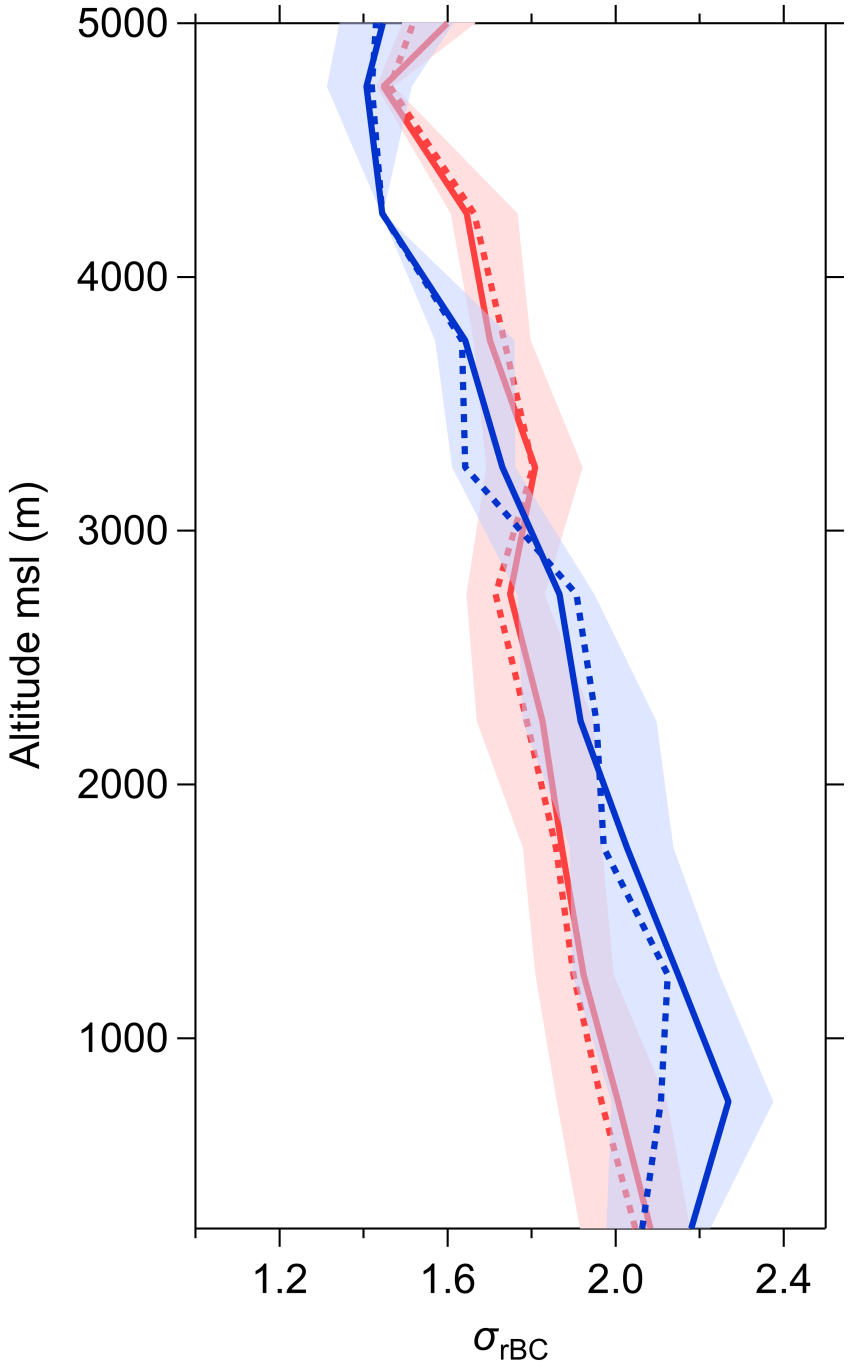

Figure S7. Vertical profiles of M_{BC} microphysical properties, the geometric standard deviation (σ_{rBC}) of the core size distributions. 2020 BLUESKY measurements in blue and 2017 EMeRGe EU measurements in red. Dashed lines show the median, solid lines the mean concentration and shaded areas represent interquartile range for each altitude bin of $500\,\mathrm{m}$.

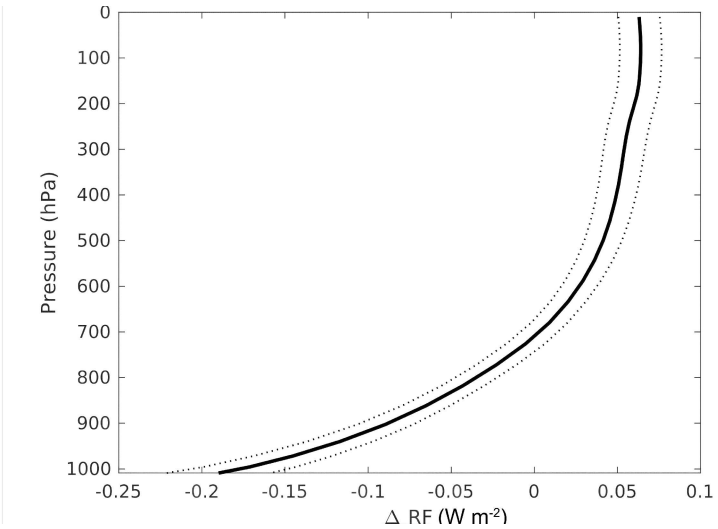

Figure S8. Profile for difference in aerosol radiative effect due to a reduction of $40\,\%$ in M_{BC}. The profile is averaged for the months May and June over the region of HALO measurements (latitude between -5 and $16°$ and longitude between 37.5 and $54.5°$, Fig. 1).

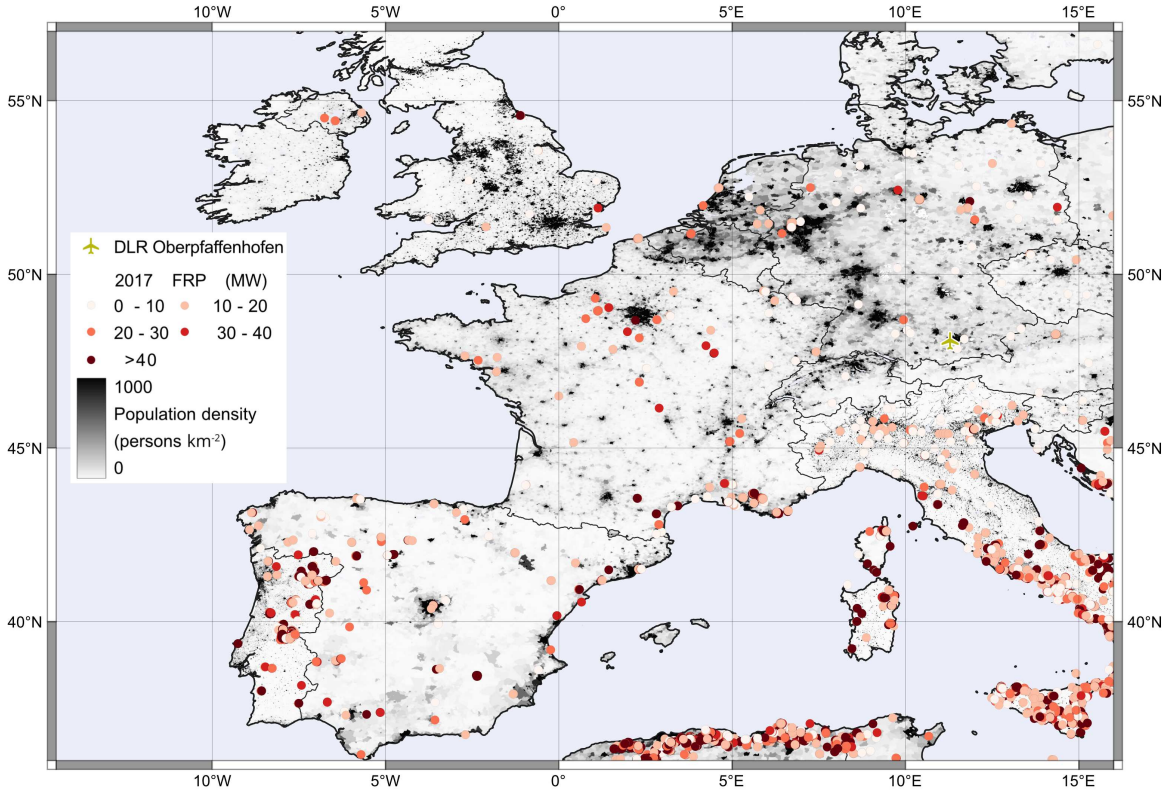

Figure S9. MODIS fires and thermal anomalies color-coded by Fire Radiative Power (FRP) in megawatts. Data was provided from https://firms.modaps.eosdis.nasa.gov/download/create.php, date of data downlaod 02.03.2022.

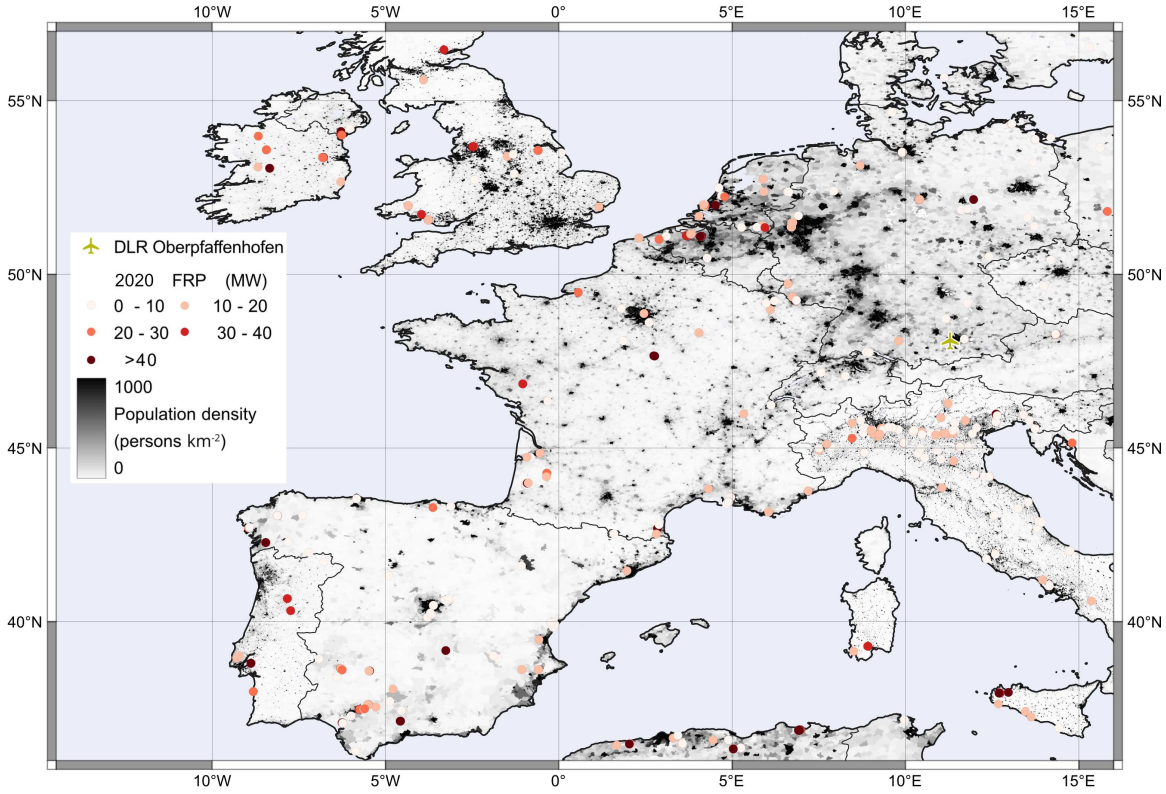

Figure S10. MODIS fires and thermal anomalies color-coded by Fire Radiative Power (FRP) in megawatts. Data was provided from https://firms.modaps.eosdis.nasa.gov/download/create.php, date of data downlaod 02.03.2022.

References

Rolph, G., Stein, A., and Stunder, B.: Real-time Environmental Applications and Display sYstem: READY, Environmental Modelling and Software, 95, 210–228, https://doi.org/10.1016/j.envsoft.2017.06.025, http://dx.doi.org/10.1016/j.envsoft.2017.06.025, 2017.

Stein, A. F., Draxler, R. R., Rolph, G. D., Stunder, B. J., Cohen, M. D., and Ngan, F.: Noaa's hysplit atmospheric transport and dispersion modeling system, Bulletin of the American Meteorological Society, 96, 2059–2077, https://doi.org/10.1175/BAMS-D-14-00110.1, 2015.